Electronic Supplementary Material (ESI) for Nanoscale.

Supplementary Information

Direct Observation of the Grain Boundary Segregation in Molybdenum Substituted Lanthanum Tungstate Membranes

Ke Ran,[a,b*] Wendelin Deibert,[c] Mariya E. Ivanova,[c] Wilhelm A. Meulenberg,[c,d] Joachim Mayer[a,b]

[a]Central Facility for Electron Microscopy GFE, RWTH Aachen University, 52074 Aachen, Germany.

[b]Ernst Ruska-Centre for Microscopy and Spectroscopy with Electrons ER-C, Forschungszentrum Jülich GmbH, 52425 Jülich, Germany.

[c]Institute of Energy and Climate Research IEK-1, Forschungszentrum Jülich GmbH, 52425 Jülich, Germany.

[d]Faculty of Science and Technology, Inorganic Membranes, University of Twente, 7500 AE Enschede, The Netherlands.

*Corresponding author E-mail: ran@gfe.rwth-aachen.de (K.R.)

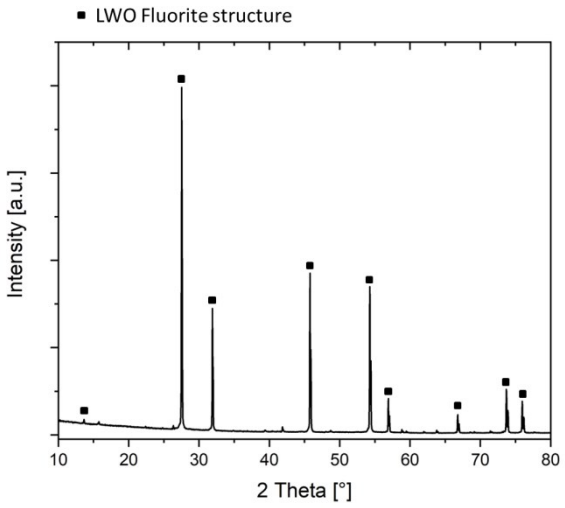

Fig. S1 XRD result of the LWO-Mo. Characteristic peaks for the LWO fluorite structure are marked.

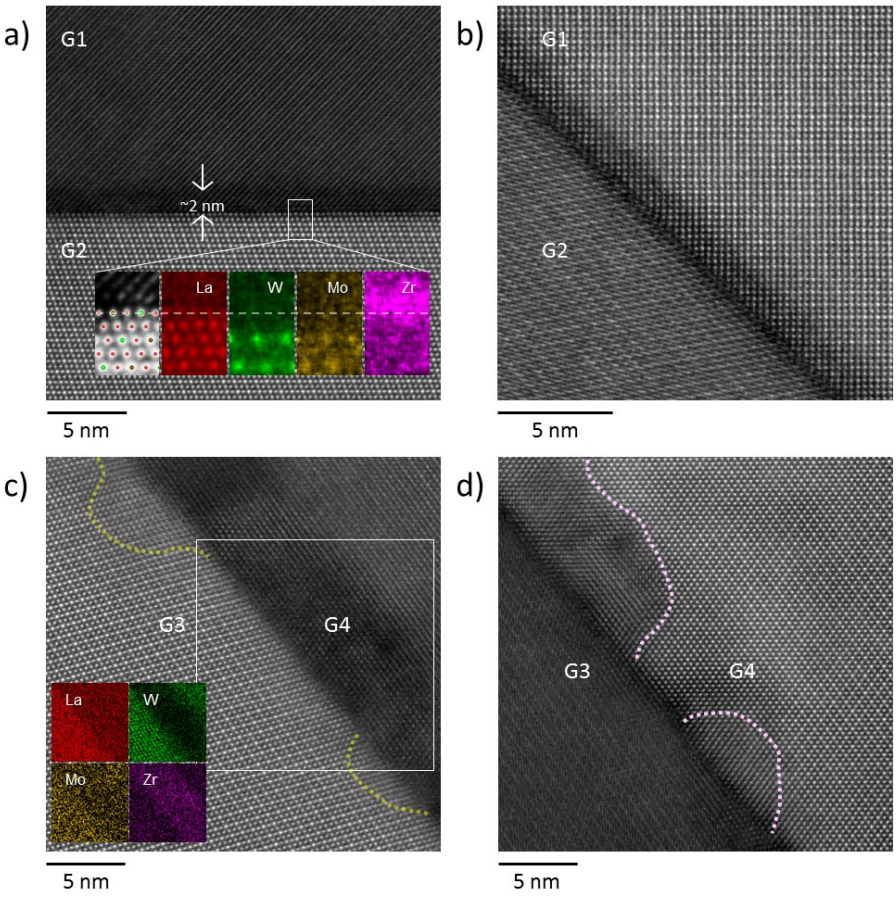

Fig. S2 (a) HAADF image taken from a same region as Fig. 2a. The lower inset shows the EDX chemical mapping results: the simultaneously acquired HAADF image compared with the average LWO model (red: La, green: W), and the elemental maps of La, W, Mo and Zr. On the G2 side, depletion of W is noticed in the first atomic plane as indicated by the dashed line. (b) HAADF image recorded from the same region as (a), with G1 oriented along the [001] direction. The G1-G2 interface showing a dark contrast is less sharp than in (a). (c-d) the interface between two LWO-Mo grains, G3 and G4, with G3/G4 oriented along the [101] direction in (c)/(d). Based on the EDX elemental maps collected from the rectangle region in (c), the dark contrast along the GB can be considered as a result of the Zr segregation. As suggested by the dotted curves, individual nanograins can be located on both sides of the GB. Clearly, structural disorders are noticed inside these nanograins.

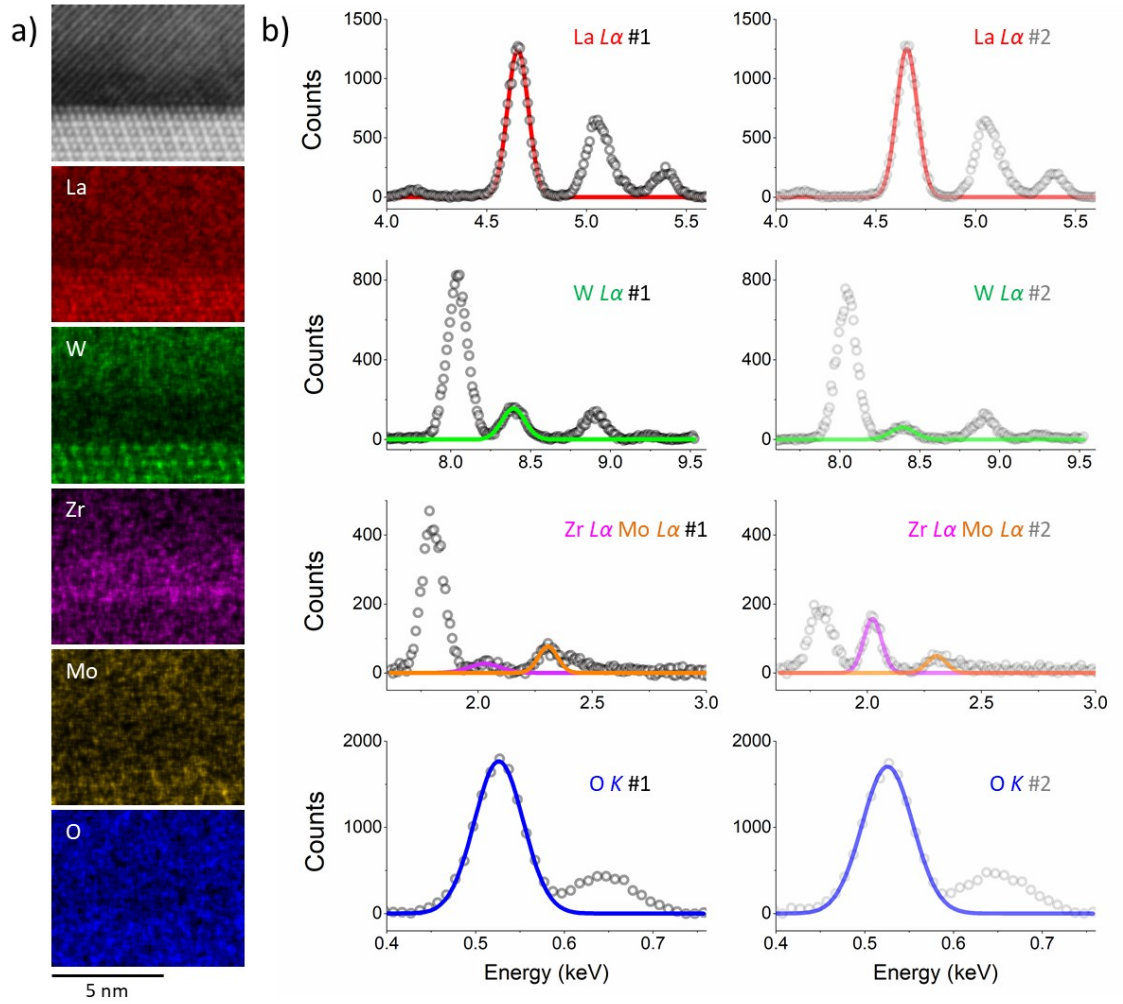

Fig.S3 (a) HAADF image and EDX elemental maps of La *Lα*, W *Lα*, Zr *Lα*, Mo *Lα* and O *K*, from the same region as shown in Fig. 2b. (b) Comparison of the unprocessed spectra (circles) and the Gaussian fitted peaks (solid lines), from region #1 (left) and #2 (right) respectively.

Determination of the secondary phase $La_6W_2O_{15}$

Inside the LWO-Mo membrane, in addition to the primary LWO-Mo phase, a few SP grains were occasionally located. The HAADF image in Fig. S4a shows an interface between a LWO-Mo and a SP grain, with the LWO-Mo oriented along the [101] direction. On the LWO-Mo side, Zr segregation is observed in the form of individual nanograins. These nanograins are around 20 nm in size, showing a hillock shape and relatively darker contrast than the LWO-Mo.

In order to identify the SP, both EDX chemical mapping and electron diffraction were utilized. The best fit with our results was found to be the $La_6W_2O_{15}$.[1] Fig. S4b shows the $La_6W_2O_{15}$ model, and the HAADF image in Fig. S4c was taken along the [012] direction. Comparing with the superimposed $La_6W_2O_{15}$ model oriented along the [012] direction in Fig. S4c, each local maximum in the HAADF image is corresponding to a cluster of atomic columns. Besides, the diffraction pattern on the lower right corner is also in a good agreement with the $La_6W_2O_{15}$ structure.

Fig. S4d shows the HAADF image of the SP along the [102] direction, and the corresponding EDX elemental maps with atomic resolution. Both HAADF image and the elemental maps fit well with the superimposed $La_6W_2O_{15}$ model along the [102] direction in Fig. S4d. In addition to the La and W, Mo and Zr were also detected, which show similar distributions as the W. Thus, the W sites inside the $La_6W_2O_{15}$ are partially occupied by Zr and Mo.

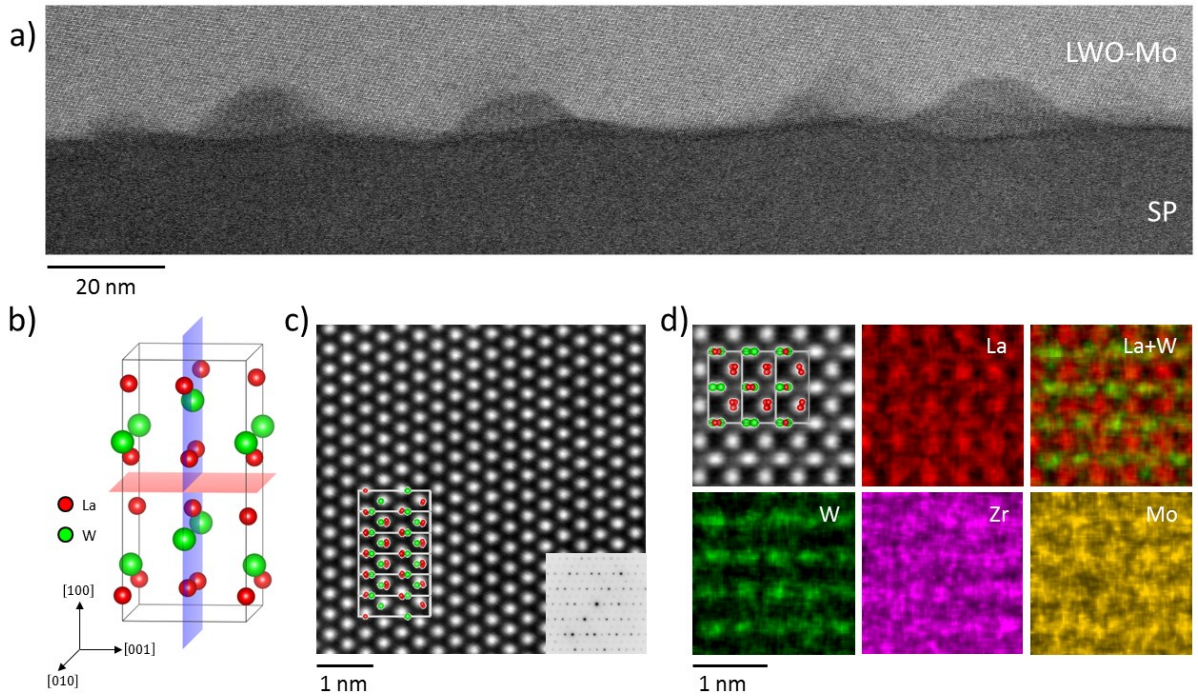

Fig. S4 (a) HAADF image showing the interface between the LWO-Mo and the SP. The LWO-Mo is oriented along the [101] direction, and the SP is determined as $La_6W_2O_{15}$. (b) the structural model of $La_6W_2O_{15}$. (c) HAADF image of the SP along [012] direction and the corresponding diffraction at the lower right corner. (d) HAADF image and the EDX elemental maps of the SP oriented along [102] direction.

The GB segregation between the LWO-Mo and the $La_6W_2O_{15}$

Fig. S5a is a closer look of one nanograin as those shown in Fig. S4a. Through a series of (-111), (11-1) and (010) planes, the nanograin is separated from the SP and the LWO-Mo. The two rectangles, marked as #1 and #2 in Fig. S5a, was selected for further EDX mapping, and Fig. S5b-c show the corresponding elemental maps. Consistent with Fig. 3d-e, all the maps in Fig. S5b show a good agreement with the LWO crystal structure, and several local maxima of Mo can be located at the W sites. The La map in Fig. S5c still follows the LWO model, but any local maximum is barely detectable in the W or Mo map. Fig. S5d compares the major peaks extracted from both mappings. Following the same method as described before, the chemical composition in region #2 was estimated by taking region #1 as an internal standard and listed in Table S1. A La/O ratio of 0.47 is obtained for the region #2, and around 35% of the W sites inside region #2 are occupied by Zr. However, the SP can also contribute to the estimated compositions for region #2, as along the viewing direction, region #2 could be a combination of the LWO-Mo, nanograin and the SP. The central squared region is used for the analysis in Fig. 5.

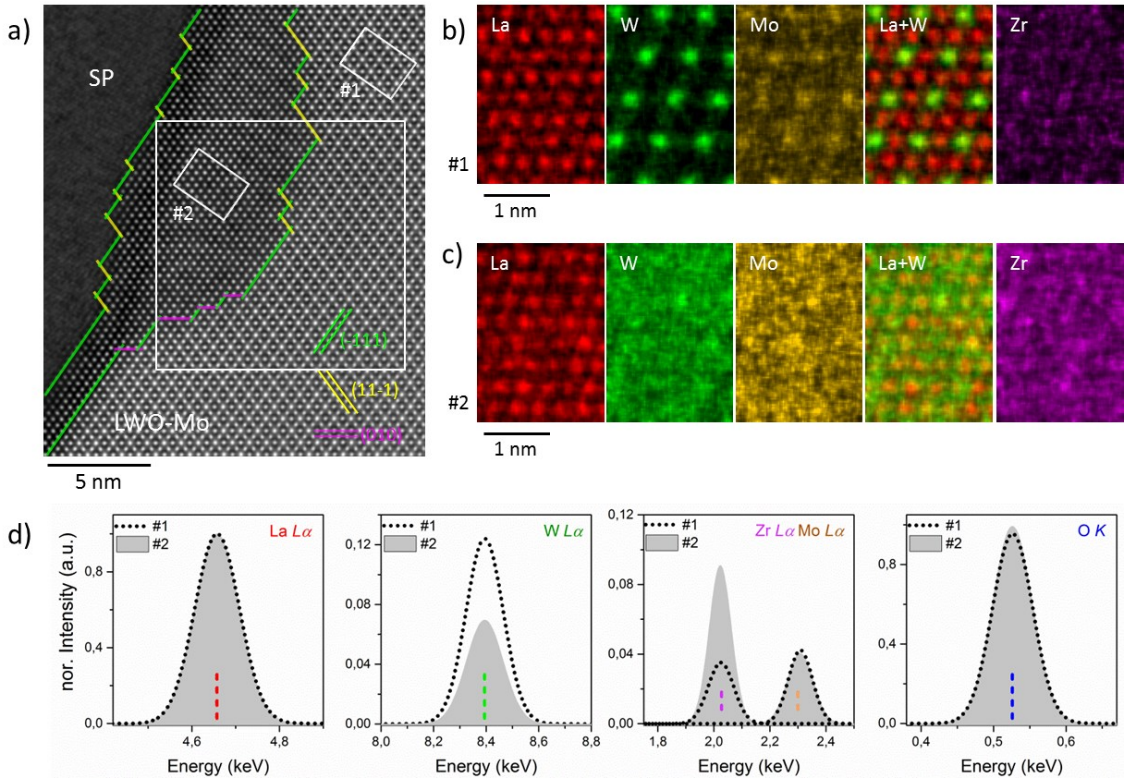

Fig. S5 (a) HAADF image showing a nanograin between the SP ($La_6W_2O_{15}$) and the LWO-Mo. The LWO-Mo is oriented along the [101] direction. (b-c) EDX elemental maps corresponding to the two rectangle, #1 and #2 defined in (a). (d) The La *La*, W *La*, Zr *La*, Mo *La* and O *K* peaks from rectangle #1 and #2, after background subtraction, normalization and fitting with Gaussian function.

at. %	La/W	La/O	W/(W+Mo+Zr)	Mo/(W+Mo+Zr)	Zr/(W+Mo+Zr)
#1	6.75	0.49	0.8	0.2	-
#2	12.17±0.42	0.47±0.01	0.44±0.02	0.21±0.02	0.35±0.04

Table S1 The estimated chemical composition for rectangle #2 in Fig. S5a, by taking region #1 as an internal standard.

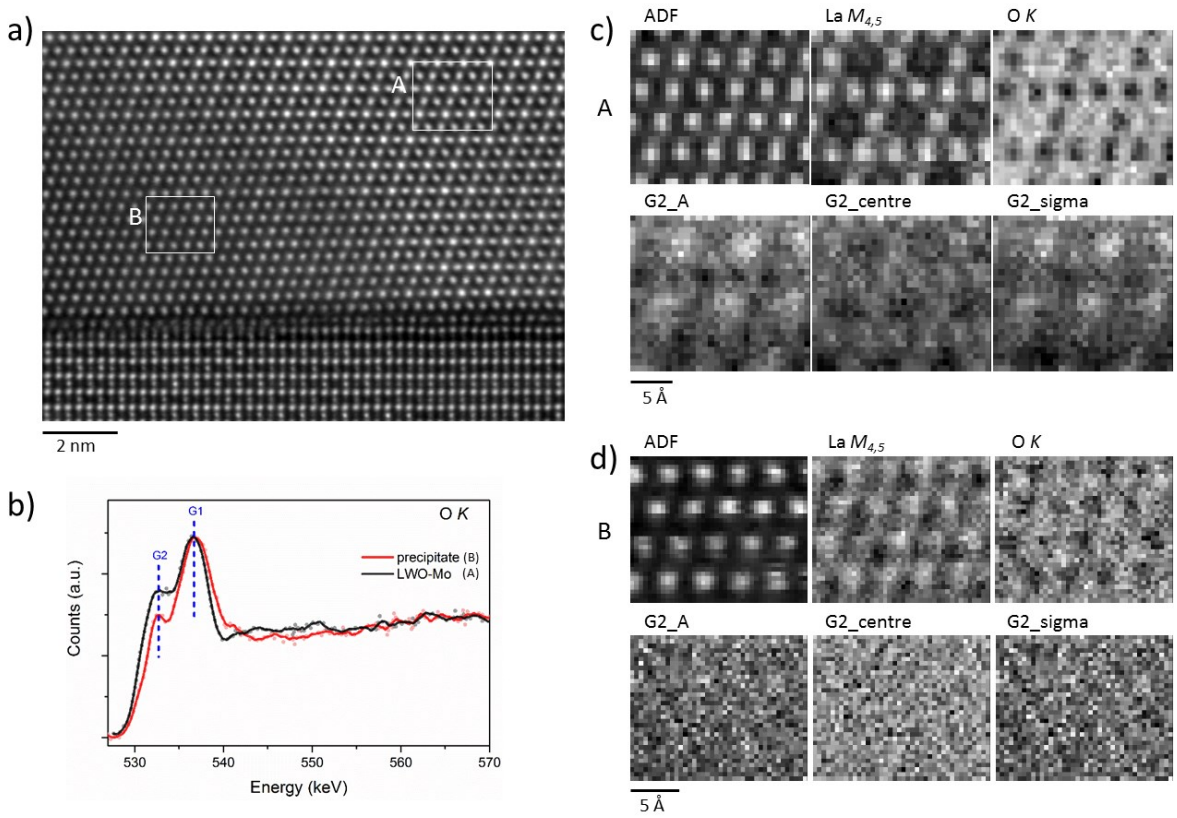

Fig. S6 (a) The HAADF image in Fig. 3b. Two regions, A and B, were selected for EELS elemental mapping. (b) The EELS spectra in Fig. 5a, collected from the region A and B as defined in (a). (c) The spectrum imaging results from region A. Top row: the simultaneously acquired annular dark-field (ADF) image and the extracted maps of La $M_{4,5}$ and O *K* edge. For the O *K* edge, both peaks G1 and G2 as labeled in (b) were fitted with Gaussian functions, $f(x) = \frac{A}{\sigma\sqrt{2\pi}} exp\left[-\frac{(x-x_0)^2}{2\sigma^2}\right]$. The G2_A, G2_centre and G2_sigma maps in the lower row are corresponding to the fitted parameters A, x_0 and σ in the Gaussian function. For all the three maps, local maxima or minima can be located at the W1 sites. (d) The spectrum imaging results from region B. Due to the substitution of W by Zr inside the nanograin, no modulation of any significance in G2_A, G2_centre or G2_sigma can be noticed.

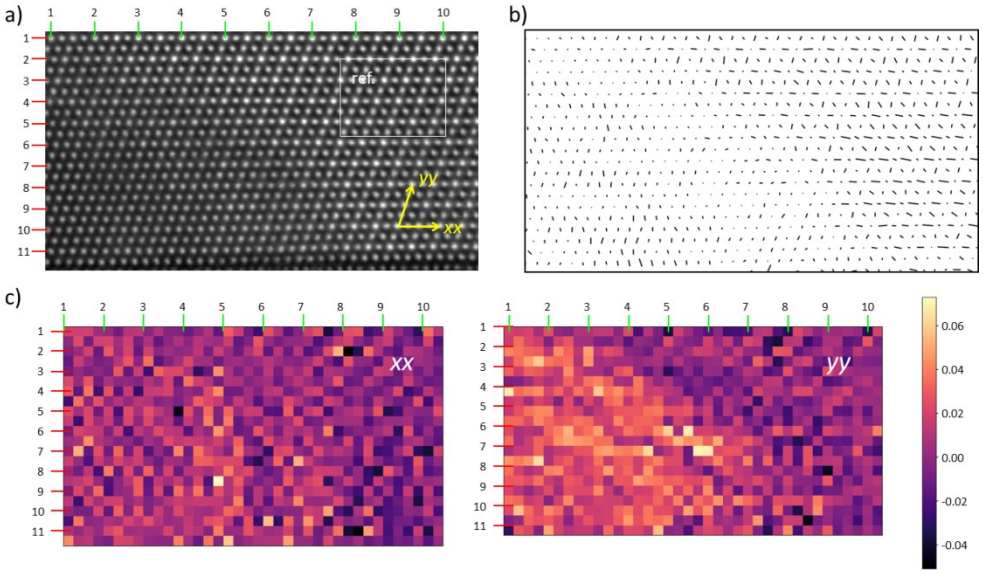

Fig. S7 (a) HAADF image cropped from Fig. 3b. (b) Mapping the ellipticity of each atomic column in (a). (c) Strain maps estimated from (a), along *xx* and *yy* directions as indicated in (a). The upper right part from the LWO-Mo was used for reference.

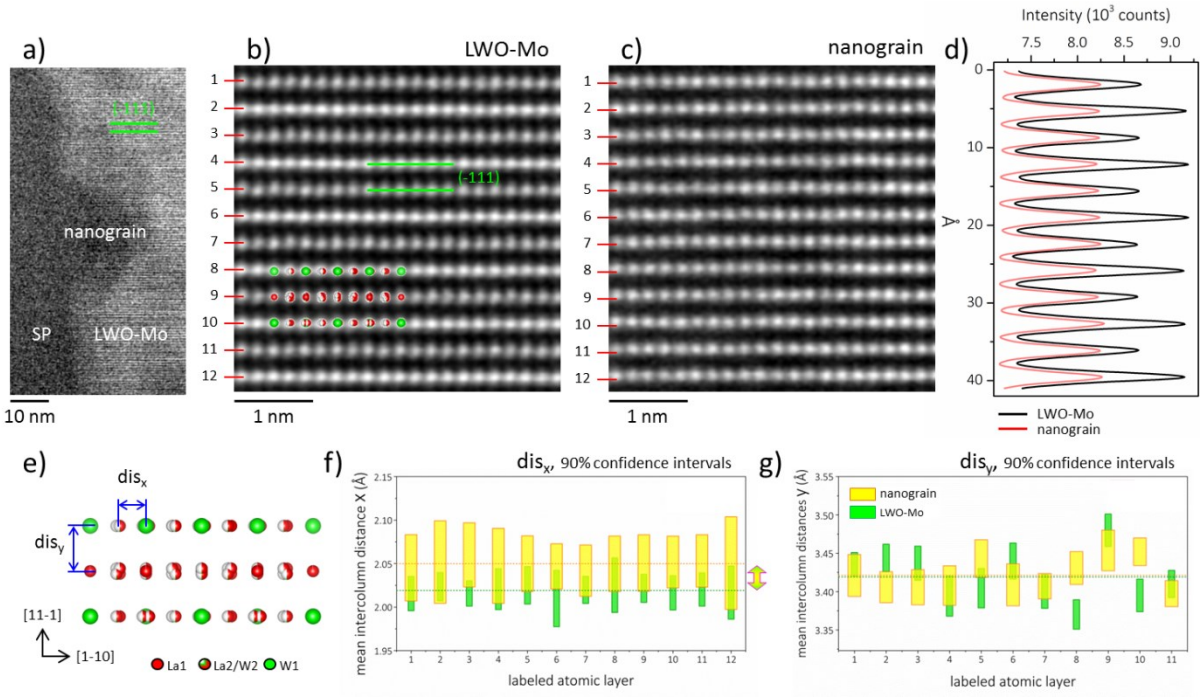

Fig. S8 (a) HAADF image with low magnification shows the SP ($La_6W_2O_{15}$), LWO-Mo and nanograin from the Zr segregation. The LWO-Mo is oriented along the [112] direction, and the parallel fringes are corresponding to the (-111) planes as indicated by the solid lines. (b-c) HAADF images of the LWO-Mo and nanograin in (a) along [112] direction. Inset in (b) is the average model of LWO along [112]. (d) Comparison of the intensity profiles along the vertical direction between (b) and (c). The nanograin shows a significantly lower intensity without any modulation. (e) Definition of dis_x and dis_y, where dis_x can be roughly considered as perpendicular to the interface while dis_y as parallel to the interface. (f-g) Measured dis_x and dis_y with their 90% confidence intervals from (b) and (c). The dotted lines indicate the mean values of dis_x and dis_y. Between the LWO-Mo and the nanograin, similar mean values of dis_y are obtained, while the averaged dis_x in nanograin is ~ 3 pm larger than that in the LWO-Mo.

1. Chambrier, M. H.; Ibberson, R. M.; Goutenoire, F. Structure Determination of α-$La_6W_2O_{15}$. *J. Solid State Chem.* **2010,** 183, 1297-1302.